Research Square

Preprints are preliminary reports that have not undergone peer review.
They should not be considered conclusive, used to inform clinical practice,
or referenced by the media as validated information.

Grape Stem Extracts from Vitis vinifera cv. Areni Noir and cv. Rkatsiteli: Rkatsiteli Shows Stronger Antiproliferative Activity and Drives BCL-2/p53-Mediated Apoptosis in MCF-7 Breast Cancer Cells

Virab Kirakosyan
Institute of Fine Organic Chemistry of Scientific - Technological Center of Organic and Pharmaceutical Chemistry
Hayarpi Javrushyan
hg.javrushyan@ysu.am
Yerevan State University
Armenuhi Mnatsakanyan
Institute of Fine Organic Chemistry of Scientific - Technological Center of Organic and Pharmaceutical Chemistry
Astghik Mkrtchyan
Yerevan State University
Andranik Davinyan
Institute of Fine Organic Chemistry of Scientific - Technological Center of Organic and Pharmaceutical Chemistry
Serkos Haroutounian
Agricultural University of Athens
Nikolay Avtandilyan
Yerevan State University

Research Article

Keywords: Grape stem extract, polyphenols, MCF-7, BCL-2/p53, molecular docking, by-product valorization

Posted Date: November 2nd, 2026

DOI: https://doi.org/10.21203/rs.3.rs-10755060/v1

License: This work is licensed under a Creative Commons Attribution 4.0 International License. Read Full License

Additional Declarations: No competing interests reported.

Abstract

Winemaking by-products from grape cultivars grown in Armenia remain an underexplored source of bioactive polyphenols with antioxidant and anticancer potential. This study compared 70% ethanolic extracts from the primary winemaking by-products of *Vitis vinifera* cv. Areni Noir and cv. Rkatsiteli, characterizing their polyphenolic composition (HPLC–MS), antioxidant activity (DPPH assay), and antiproliferative effects in MCF-7 breast cancer cells (MTT, real-time cell analysis). HPLC–MS revealed a diverse profile of flavonoids, flavan-3-ols, hydroxycinnamic acids, stilbenes, and triterpenoids in both cultivars, with Rkatsiteli particularly rich in catechin and caftaric acid, and Areni Noir higher in gallic acid. Antioxidant activity was comparable between extracts (DPPH IC_{50} ≈183–189 μg/mL). In MCF-7 cells, both extracts reduced cell growth, but Rkatsiteli produced the stronger antiproliferative response and was therefore selected for downstream mechanistic analysis: it increased SOD activity, elevated MDA, and reduced catalase activity, indicating a controlled oxidative stress response, and markedly downregulated BCL-2 while upregulating p53, consistent with activation of pro-apoptotic signaling. Molecular docking identified ε-viniferin, oleanolic acid, and polydatin as promising ligands for BCL-2 and p53, with oleanolic acid and polydatin combining strong predicted affinity with more favorable ADMET profiles. These findings position Rkatsiteli grape stem extract as a particularly promising source of natural antiproliferative compounds warranting further preclinical investigation.

1. INTRODUCTION

During winemaking, substantial solid waste is generated worldwide: grape pomace and stems account for approximately 20–30% of processed grape weight, corresponding to roughly 200–300 kg of waste per ton of grapes [1]. Global wine production (225–258 million hectoliters annually) generates millions of tons of winery residues, posing environmental challenges [2]. In Armenia, approximately 280,000 tons of grapes are processed annually by around 130 wineries, generating nearly 45,000 tons of waste that is frequently discarded without adequate processing, creating risks of soil and water contamination. Interest in grape-derived bioactive compounds grew after the "French paradox" linked moderate red wine consumption to reduced cardiovascular disease risk, largely attributed to polyphenols [3]. Grape by-products are now recognized as valuable sources of polyphenols with antioxidant, anti-inflammatory, antimicrobial, and anticancer properties [4–7], and grape-derived compounds such as resveratrol, catechins, and procyanidins can modulate pathways associated with oxidative stress, apoptosis, and tumor progression [8–11]. Breast cancer remains among the most prevalent and lethal malignancies, and its progression involves dysregulated oxidative stress and apoptosis, particularly through the anti-apoptotic regulator BCL-2 and the tumor suppressor p53 [12–16]. Identifying natural compounds that modulate these targets is thus an active area of anticancer research [17]. However, studies integrating phytochemical characterization, antioxidant assessment, in vitro anticancer evaluation, oxidative stress and apoptosis analysis, and computational approaches remain scarce for grape by-products, and comparative data on Armenian cultivars are lacking [1, 9].

This study therefore compared 70% ethanolic extracts of the endemic Armenian cultivar *Vitis vinifera* cv. Areni Noir and cv. Rkatsiteli by HPLC-MS profiling and DPPH antioxidant analysis, followed by evaluation of antiproliferative activity in MCF-7 breast cancer cells (MTT, RTCA), oxidative stress markers, and apoptosis-related proteins (BCL-2, p53). Molecular docking was performed to explore interactions between major identified compounds and these targets. The novelty lies in integrating phytochemical, experimental, and computational approaches to evaluate the anticancer potential of Armenian grape-derived polyphenols.

2. METHODS

2.1. Preparation of the Sample Solution

Grape stems of *Vitis vinifera* L. cv. Areni Noir and cv. Rkatsiteli were obtained after the 2025 harvest from AreWine LLC (Areni, Vayots Dzor, Armenia) and "ARM VINO" (Norabac, Ararat Province, Armenia), respectively. Stems were air-dried in the

dark, milled, and stored at room temperature. Ground material was cold-macerated with 70% (v/v) ethanol (1:10 w/v) in a water bath at 38–40°C for 5 h with continuous stirring, then filtered and used for phytochemical and biological assays.

2.2. Chemicals and Standards

Analytical-grade $K_3Fe(CN)_6$, $FeCl_3 \cdot 6H_2O$, HCl, $AlCl_3 \cdot 6H_2O$, and $CH_3COONa \cdot 3H_2O$ were from Sigma-Aldrich/Merck (Germany); HPLC-grade methanol, ethanol, and acetonitrile were from VWR, and LC-MS-grade formic acid from Sigma-Aldrich. Reference standards were rutin trihydrate (Fluka), chlorogenic acid (Thermo Scientific), and gallic acid monohydrate (Sigma-Aldrich). MTT assay reagents, DMEM, FBS, and antibiotics were from Sigma-Aldrich; cell-culture supplements from Thermo Fisher (Gibco). RTCA E-plates and consumables were from Agilent Technologies, used with the xCELLigence RTCA eSight system per manufacturer instructions.

2.3. LC–MS Analysis

Phenolics were analyzed by Xevo™ QToF MS coupled to an ACQUITY UPLC system (Waters) with PDA detection, in negative ESI mode (cone voltage 20–60 V) [1, 2]. Separation used an ACQUITY™ Premier BEH C18 column (1.7 µm, 2.1 x 50 mm), water/acetonitrile mobile phases, and a multistep gradient (0.3 mL/min, 30°C; 0–2 min 95:5 A:B, ramping to 90% B by 18 min, then re-equilibration to 95:5 by 25 min). Compounds were identified against reference standards' retention times and mass spectra. Flavonoids, phenylpropanoids, and total phenolics were quantified against rutin (R^2=0.9990), chlorogenic acid (R^2=0.9934), and gallic acid (R^2=0.9944) calibration curves, respectively. MS conditions: source 120°C, desolvation gas 450°C, capillary 3.0 kV, cone/desolvation gas flow 50/850 L/h, scan time 0.5 s, mass range 50-1200 Da; data acquired with MassLynx software, identification based on exact molecular mass. Although oleanolic acid is a triterpenoid rather than a phenolic compound, it was detected and quantified under the same LC-MS run and is reported alongside the phenolic constituents for completeness.

2.4 Quantification of Total Polyphenols and Flavonoids Content

Total phenolic content (TPC) was determined using a spectrophotometric method based on the Prussian Blue color reaction, which measures the reducing capacity of polyphenols [3]. A calibration curve of gallic acid (R^2 = 0.9907) was employed, and results were expressed as mg gallic acid equivalents (GAE) per g of dried plant material. Total flavonoid content (TFC) was measured spectrophotometrically using the aluminum chloride method [4], with a calibration curve of rutin (R^2 = 0.9977). Results were expressed as mg rutin equivalents (RE) per g of dried plant material.

2.5 DPPH Radical Scavenging Activity

Antioxidant capacity was measured by the DPPH radical scavenging assay. Dried, ground stems were extracted with 70% ethanol and diluted 2-25x. Diluted extract (varying volumes) was mixed with 2 mL of 0.15 mg/mL DPPH in methanol and incubated at 40°C for 30 min; absorbance was read at 517 nm. Inhibition (%) = (A(control) - A(sample))/A(control) x 100, and results expressed as IC_{50} (µg/mL) [5].

2.6 Cell cultures

Human breast adenocarcinoma MCF-7 (cat. # HTB-22) cell culture was obtained from ATCC and maintained in DMEM medium supplemented with L-glutamine (2 mmol/L), sodium pyruvate (200 mg/L), fetal bovine serum (100 mL/L), and antibiotics (100 U/mL penicillin and 100 µg/L streptomycin). Cells were grown at 37°C under a humidified atmosphere with 5% CO2 in a Biosmart (Biosan, Latvia) as described before [6]. Cultured cells were regularly examined for the presence of mycoplasma contamination using the Universal Mycoplasma Detection Kit from ATCC (Manassas, Virginia, USA).

2.7 MTT cytotoxicity test

The inhibitory effects of the Vitis vinifera L. Cv. Areni Noir and Vitis vinifera L. Cv. Rkatsiteli extracts on the proliferation of the MCF-7 cell line were assessed using the MTT assay, as previously detailed [7]. The assay was performed in three

separate experiments, each containing four technical replicates. Cytotoxicity was determined by calculating the percentage of growth inhibition in cells treated with the grape extract compared to control cells treated only with the solvent (resulting in a final concentration of 1% ethanol), which was designated as 100% growth.

2.8. Impedance-based real-time cell monitoring and cytotoxicity assessment

MCF-7 cells (10,000/well) were seeded in E-Plate 96 wells on an Agilent xCELLigence RTCA eSight system; background impedance was recorded before seeding, then cells were added (final 200 µL/well) and allowed to settle (30 min, room temperature) before 24 h incubation (37°C, 5% CO_2). Cell index was recorded every 15 min for 96 h, normalized to t = 0, with Rkatsiteli extract (0.5 mg/mL) added at 24 h; vehicle-treated wells served as controls (mean ± SD, n = 3) [7].

2.9. Acquisition and analysis of protein structures

Bcl-2 (PDB: 4MAN) and p53 (PDB: 1TSR) crystal structures were retrieved from the Protein Data Bank and processed in PyMOL (Schrodinger) [8], removing solvents, ions, and non-protein components; ligands were separated for re-docking, and refined protein models were used for docking.

2.10. Enhanced molecular docking using AutoDock Vina

Docking was performed with AutoDock Vina (exhaustiveness = 16) [9], and interaction diagrams (hydrogen bonds, hydrophobic contacts, π–π interactions, residues) were generated with BIOVIA Discovery Studio.

2.11. Oxidative stress enzymes

The catalase activity in different tissues was measured by the titration method and expressed as the µmol of hydrogen peroxide broken down in 1 mg of protein [6]. Peroxidase activity was determined according to the spectroscopic method. The activity of peroxidase was expressed in µmol/min/mg protein. Superoxide dismutase (SOD) activity of different tissues was measured according to the degree of inhibition of the adrenaline self-oxidation reaction rate, as shown before. SOD activity was expressed in conventional units of activity 50% inhibition. The reaction was taken as 1 conventional unit of enzyme activity.

2.12. Immunocytochemistry (ICC)

MCF-7 cells (96-well black plates) were treated with DMSO (control) or Rkatsiteli extract (0.5 mg/mL, 24 h) [29], fixed (4% PFA), permeabilized (1% Triton X-100), blocked (1% BSA), and incubated with primary antibodies (BCL-2, p53; 1:250) overnight at 4°C, then Alexa Fluor 647-labeled anti-rabbit IgG (1:500) and DAPI nuclear stain. Images were acquired on a Cytation C10 confocal microscope (20x objective) and analyzed with Gen5 software.

2.13. Statistical analysis

Results are presented as means ± SEM. We analyzed the data using one-way ANOVA; Tukey's test was employed to evaluate the statistical significance of the results for MDA, SOD, Catalase, BCL-2, and p53. DPPH, TPC, TFC, and MTT viability data were analyzed by one-way ANOVA with Tukey's post hoc test using the same software and significance threshold. Statistical analyses were performed using GraphPad Prism 8 software (San Diego, CA, USA), and a significance level of $p < 0.05$ was deemed statistically significant.

3. RESULTS

3.1.HPLC-DAD-ESI Analysis

HPLC-DAD-ESI analysis (Tables 1 and 2) revealed a complex phenolic composition in both grape stem extracts, dominated by hydroxycinnamic acids, flavan-3-ols, flavonols, stilbenes, and phenolic acids, consistent with previous reports on grape

stems as rich polyphenol sources [26–29]. Areni Noir (indigenous Armenian red variety) and Rkatsiteli (white variety of Georgian origin, widely grown in Armenia) shared a similar qualitative profile — caftaric, caffeic, coutaric, fertaric, gallic, coumaric, cinnamic, protocatechuic, and syringic acids; catechin, epicatechin, and procyanidins B1/B2; quercetin and kaempferol derivatives; and the stilbenes resveratrol, polydatin, and ε-viniferin — but differed markedly in relative abundance.

Table 1
Quantification and identification of phenolic compounds (mg/kg dry vegetal product) in the 70% ethanolic extract of primary winemaking by-products of Rkatsiteli grape variety by HPLC-DAD-ESI$^-$ analysis

N	Compound name	Chemical Formula	Theoretical M/z	Acquired M/z	Mass Error	Rt	Mean Area	Standard	Quantity mg/kg
1.	**Caftaric acid**	**$C_{13}H_{12}O_9$**	**311.0403**	**311.0415**	**-3.86**	**2.07**	**125292**	**Chlorogenic acid**	**110.51 ± 0.56**
2.	Caffeic acid	$C_9H_8O_4$	179.0344	179.0350	-3.35	2.59	37799	-	N.q.
3.	Coutaric acid	$C_{13}H_{12}O_8$	295.0454	295.0466	-4.07	2.96	37918	-	N.q.
4.	Gallic acid	$C_7H_6O_5$	169.0137	169.0141	-2.37	3.30	4355	Gallic acid	2.49 ± 0.06
5.	Fertaric acid	$C_{14}H_{14}O_9$	325.0560	325.0569	-2.77	4.33	36220	Chlorogenic acid	4.38 ± 0.03
6.	Procyanidin B1	$C_{30}H_{26}O_{12}$	577.1346	577.1346	0	5.21	165102	-	N.q.
7.	Coumaric acid	$C_9H_8O_3$	163.0395	163.0399	-2.45	5.52	1808	-	N.q.
8.	Catechine	$C_{15}H_{14}O_6$	289.0712	289.0725	-4.50	5.70	345684	Chlorogenic acid	107.43 ± 0.12
9.	Procyanidin B2	$C_{30}H_{26}O_{12}$	577.1346	577.1346	0	6.38	51878	-	N.q.
10.	Myricetin	$C_{15}H_{10}O_8$	317.0298	317.0308	-3.15	7.03	3279	-	N.q.
11.	Cinnamic acid	$C_9H_8O_2$	147.0446	147.0453	-4.76	7.04	2917	Gallic acid	0.53 ± 0.02
12.	Epicatechin	$C_{15}H_{14}O_6$	289.0712	289.0726	-4.84	7.14	53246	Chlorogenic acid	16.68 ± 0.17
13.	Protocatechuic acid	$C_7H_6O_4$	153.0188	153.0195	-4.57	7.44	2320	Gallic acid	0.11 ± 0.01
14.	Syringic acid	$C_9H_{10}O_5$	197.0450	197.0451	-0.51	7.95	576	Gallic acid	0.056 ± 0.002
15.	Epicatechin gallate	$C_{22}H_{18}O_{10}$	441.0822	441.0829	-1.59	8.34	79985	Gallic acid	7.94 ± 0.03
16.	Quercetin-3-β-D-glucoside	$C_{21}H_{20}O_{12}$	463.0876	463.0888	-2.60	9.69	158914	Rutin	19.91 ± 0.04
17.	Rutin	$C_{27}H_{30}O_{16}$	609.1456	609.1456	0	9.79	60734	Rutin	2.73 ± 0.03
18.	Resveratrol	$C_{14}H_{12}O_3$	227.0708	227.0718	-4.40	10.04	5129		N.q.
19.	Polydatin	$C_{20}H_{22}O_8$	389.1237	389.1245	-2.06	10.52	3512	Chlorogenic acid	0.015 ± 0.0006
20.	Kaemferol 7-O-glicoside	$C_{21}H_{20}O_{11}$	447.0927	447.0945	-4.03	10.62	57627	Rutin	12.12 ± 0.05
21.	Kaemferol 7-O-rutinoside	$C_{27}H_{30}O_{15}$	593.1506	593.1511	-0.84	10.74	21991	Rutin	0.085 ± 0.003
22.	ε-Viniferin	$C_{28}H_{22}O_6$	453.1338	453.1351	-2.87	11.66	111013	-	N.q.

Note: N.q = Not quantified

N	Compound name	Chemical Formula	Theoretical M/z	Acquired M/z	Mass Error	Rt	Mean Area	Standard	Quantity mg/kg
1.	**Caftaric acid**	**$C_{13}H_{12}O_9$**	**311.0403**	**311.0415**	**-3.86**	**2.07**	**125292**	**Chlorogenic acid**	**110.51 ± 0.56**
23.	Quercetin	$C_{15}H_{10}O_7$	301.0348	301.0359	-3.65	11.90	54260	-	N.q.
24.	Kaempferol	$C_{15}H_{10}O_6$	285.0399	285.0411	-4.21	12.82	6455	-	N.q.
25.	Oleanolic acid	$C_{30}H_{48}O_3$	455.3525	455.3537	-2.64	20.13	792210	-	N.q.
Note: N.q = Not quantified									

Table 2
Quantification and identification of phenolic compounds (mg/kg dry vegetal product) in the 70% ethanolic extract of primary winemaking by-products of Areni grape variety by HPLC-DAD-ESI$^-$ analysis

N	Compound name	Chemical Formula	Theoretical M/z	Acquired M/z	Mass Error	Rt	Mean Area	Standard	Quantity mg/kg
1.	**Caffeic acid**	**$C_9H_8O_4$**	**179.0344**	**179.0349**	**-2.79**	**1.72**	**36091**	**-**	**N.q.**
2.	Gallic acid	$C_7H_6O_5$	169.0137	169.0143	-3.55	2.19	35709	Gallic acid	20.07 ± 0.05
3.	Caftaric acid	$C_{13}H_{12}O_9$	311.0403	311.0415	-3.86	2.45	132790	Chlorogenic acid	117.56 ± 0.13
4.	Coutaric acid	$C_{13}H_{12}O_8$	295.0454	295.0466	-4.07	3.06	40656	-	N.q.
5.	Fertaric acid	$C_{14}H_{14}O_9$	325.0560	325.0569	-2.77	4.29	51026	Chlorogenic acid	6.21 ± 0.04
6.	Procyanidin B1	$C_{30}H_{26}O_{12}$	577.1346	577.1346	0	5.10	156517	-	N.q.
7.	Coumaric acid	$C_9H_8O_3$	163.0395	163.0398	-1.84	5.74	2879	-	N.q.
8.	Catechine	$C_{15}H_{14}O_6$	289.0712	289.0724	-4.15	6.10	170871	Chlorogenic acid	53.13 ± 0.05
9.	Procyanidin B2	$C_{30}H_{26}O_{12}$	577.1346	577.1346	0	6.63	57212	-	N.q.
10.	Cinnamic acid	$C_9H_8O_2$	147.0446	147.0453	-4.76	6.98	4828	Gallic acid	0.837 ± 0.006
11.	Myricetin	$C_{15}H_{10}O_8$	317.0298	317.0309	-3.50	7.05	9840	-	N.q.
12.	Protocatechuic acid	$C_7H_6O_4$	153.0188	153.0192	-2.61	7.40	691	Gallic acid	0.032 ± 0.001
13.	Epicatechin	$C_{15}H_{14}O_6$	289.0712	289.0726	-4.84	7.49	31035	Chlorogenic acid	9.69 ± 0.046
14.	Syringic acid	$C_9H_{10}O_5$	197.0450	197.0457	-3.55	7.77	858	Gallic acid	0.084 ± 0.001
15.	Epicatechin gallate	$C_{22}H_{18}O_{10}$	441.0822	441.0830	-1.81	8.34	25690	Gallic acid	2.52 ± 0.03
16.	Polydatin	$C_{20}H_{22}O_8$	389.1237	389.1245	-2.06	8.48	4052	Chlorogenic acid	0.019 ± 0.0006
17.	Quercetin-3-β-D-glucoside	$C_{21}H_{20}O_{12}$	463.0876	463.0888	-2.60	9.65	136505	Rutin	17.08 ± 0.08
18.	Rutin	$C_{27}H_{30}O_{16}$	609.1456	609.1454	0.33	9.88	23836	Rutin	1.073 ± 0.021
19.	Resveratrol	$C_{14}H_{12}O_3$	227.0708	227.0704	1.76	10.27	4680		N.q.
20.	Kaemferol 7-O-glicoside	$C_{21}H_{20}O_{11}$	447.0927	447.0945	-4.03	10.63	57627	Rutin	11.30 ± 0.035
21.	Kaemferol 7-O-rutinoside	$C_{27}H_{30}O_{15}$	593.1506	593.1511	-0.84	10.73	14184	Rutin	0.056 ± 0.004
22.	ε-Viniferin	$C_{28}H_{22}O_6$	453.1338	453.1351	-2.87	11.83	43652	-	N.q.

Note: N.q = Not quantified

N	Compound name	Chemical Formula	Theoretical M/z	Acquired M/z	Mass Error	Rt	Mean Area	Standard	Quantity mg/kg
1.	**Caffeic acid**	**$C_9H_8O_4$**	**179.0344**	**179.0349**	**-2.79**	**1.72**	**36091**	**-**	**N.q.**
23.	Quercetin	$C_{15}H_{10}O_7$	301.0348	301.0359	-3.65	12.29	172699	-	N.q.
24.	Kaempferol	$C_{15}H_{10}O_6$	285.0399	285.0410	-3.86	13.42	52803	-	N.q.
25.	Oleanolic acid	$C_{30}H_{48}O_3$	455.3525	455.3537	-2.64	20.18	685443	-	N.q.
Note: N.q = Not quantified									

Caftaric acid was the major phenolic in both cultivars (Areni Noir 117.56 ± 0.13 mg/kg; Rkatsiteli 110.51 ± 0.56 mg/kg), consistent with its known dominance in grape stems [26, 28]. Areni Noir contained substantially more gallic acid (20.07 ± 0.05 vs. 2.49 ± 0.06 mg/kg), a compound associated, together with catechin and epicatechin, with elevated antioxidant activity within the phenolic matrix. Rkatsiteli, in contrast, was markedly enriched in flavan-3-ols — catechin (107.43 ± 0.12 mg/kg), epicatechin (16.68 ± 0.17 mg/kg), and epicatechin gallate (7.94 ± 0.03 mg/kg) — compounds strongly linked to antioxidant activity in grape stems [27–29]. Flavonol derivatives (quercetin-3-β-D-glucoside, rutin, kaempferol glycosides) were also slightly higher in Rkatsiteli, likely reflecting cultivar- and environment-dependent accumulation [28], while stilbenes, including the biologically active ε-viniferin, were present in both extracts. This pattern points to clear varietal complementarity: Areni Noir as a source of phenolic acids and Rkatsiteli as a stronger source of flavan-3-ol/flavonoid antioxidants — a distinction that anticipates the differential bioactivity observed in subsequent assays (Sections 3.5–3.7).

3□2 Quantification of total polyphenolic (TPC), flavonoids (TFC) content

The 70% ethanolic extracts prepared from the primary winemaking by-products of *Vitis vinifera* cv. Rkatsiteli and Areni were characterized for their total polyphenolic content (TPC) and total flavonoid content (TFC). The obtained results demonstrate that both extracts contain significant amounts of these bioactive compounds, which can be correlated with the biological activities assessed in this study□ According to Table 3, the Rkatsiteli extract showed a TPC value of 1.96 mg GAE/g and a TFC value of 0□4 mg RE/g, while the Areni extract exhibited slightly higher contents, with 2.15 mg GAE/g for TPC and 0□81 mg RE/g for TFC. These findings indicate a rich phenolic profile in both grape varieties, with Areni displaying a comparatively higher accumulation of total polyphenols and flavonoids.

Table 3
Total polyphenols and flavonoids content of the 70% ethanolic extracts from the primary winemaking by-products of Rkatsiteli and Areni grape varieties

N	Sample	TPC(mgGAE/g)	TFC(mgRE/g)
1.	**Rkatsiteli**	**1.96 ± 0.09**	**0□40 ± 0.04**
2.	Areni	2.15 ± 0.045	0□81 ± 0.07
Note:TFC=total flavonoids content; RE=rutin equivalents, TPA=total phenolic acids content; GAE=gallic acid equivalents□			

3□3. Antioxidant activity assay

Antioxidant activity of the extracts was assessed by DPPH radical scavenging assay across a dilution series (Table 4). Both extracts showed clear dose-dependent scavenging: Areni ranged from 17.87% (0.04 mg/mL) to 97.61% (0.6 mg/mL), and Rkatsiteli from 18.60% to 97.97% over the same range, with IC_{50} values of 188.8 and 182.9 µg/mL, respectively, indicating slightly higher efficiency for Rkatsiteli (e.g., 93.08% vs. 86.35% inhibition at 0.4 mg/mL). These results indicate that both by-

products are valuable natural antioxidant sources [2, 10], consistent with their phenolic composition [11, 12], and that antioxidant capacity may partly underlie the observed cytotoxic activity [13].

Table 4
Antioxidant activity of 70% ethanolic extracts from primary winemaking by-products of Rkatsiteli and Areni.

N	Sample	DPPH (IC50 µg/mL)
1.	**Rkatsiteli**	**182.9 ± 0.3**
2.	Areni	188.8 ± 0.2

3.4. Molecular Docking analysis of E-Viniferin, Polydatin, and Oleanolic acid with p53 and Bcl-2 proteins

A panel of natural compounds was screened for binding affinity toward p53 and Bcl-2, followed by ADMET-based pharmacokinetic/toxicity prediction, selecting compounds by combined binding affinity, ADMET profile, and efficacy-safety balance. ε-Viniferin showed the strongest binding to both proteins (Bcl-2: -8.327 kcal/mol; p53: -5.345 kcal/mol) but a less favorable ADMET profile (elevated hepatotoxicity/genotoxicity risk). Oleanolic acid combined strong affinity (Bcl-2: -7.877 kcal/mol; p53: -5.462 kcal/mol) with a more favorable safety profile (low carcinogenicity, moderate toxicity), while polydatin showed comparable affinity (Bcl-2: -7.876 kcal/mol; p53: -5.306 kcal/mol) with acceptable pharmacokinetics. These three compounds were therefore selected for detailed binding-mode analysis, representing maximal affinity (ε-viniferin), optimal affinity-safety balance (oleanolic acid), and an affinity-pharmacokinetics compromise (polydatin).

All three compounds interacted favorably with both Bcl-2 (Fig. 1) and p53 (Fig. 2) via hydrogen bonding, hydrophobic and π-mediated contacts, and van der Waals forces. In p53, ε-viniferin occupied a mixed hydrophobic-electrostatic pocket within the DNA-binding domain (residues including Ser94-96, Val97, Ser99, Gln100, Lys101, Met169, Thr170; -5.345 kcal/mol). Polydatin bound more strongly to p53 (-7.876 kcal/mol), anchored by hydrogen bonds with Thr102 and Ser269, plus π–cation (Lys101), π–sulfur (Met169), and amide–π (Pro98, Ser99) contacts. Oleanolic acid formed a key hydrogen bond with Gln100 and further hydrophobic contacts (Arg267, Arg213, Met169, Val97, Ile162, Lys101), fitting the pocket without steric clash.

Within Bcl-2, ε-viniferin occupied a hydrophobic cavity (Tyr199, Phe195, Phe101, Tyr105, Val145, Ala146, Arg143), dominated by π–π stacking with Tyr199 and π–alkyl contacts. Polydatin engaged a heterogeneous site (Asp108, Arg104, Arg143, Tyr105, Phe101, Val145, Ala146, Gly142, Asn140) via hydrophobic, π-mediated and electrostatic interactions. Oleanolic acid bound a hydrophobic groove (Phe101, Tyr105, Asp108, Val145, Ile144, Trp141; -7.877 kcal/mol) stabilized by hydrogen bonds and extensive hydrophobic/π–alkyl contacts. Collectively, all three phytochemicals form favorable predicted complexes with both targets; while ε-viniferin had the highest affinity, its toxicity profile may limit translational potential, whereas oleanolic acid and polydatin combined strong binding with more favorable ADMET characteristics. Table 5 summarizes physicochemical parameters (MW, HBA, HBD, LogP), Lipinski Ro5 drug-likeness, and docking affinities for Bcl-2 and p53.

Table 5
Physicochemical properties, Lipinski's rule of five (Ro5) evaluation, and molecular docking scores of selected ligands against Bcl-2 and p53 proteins.

Caffeic acid	**MW**	**HBA**	**HBD**	**LogP**	**Ro5**	**Bcl-2**	**p-53**
	180,04	**4**	**3**	**1,19**	**0**	**-6,045**	**-4,122**
Caftaric Acid	312,05	9	5	-0,046	0	-6,56	-4,66
Catechine	290,08	6	5	1,173	0	-6,981	-5
Cinnamic acid	148,05	2	1	2,619	0	-5,594	-4,655
Coumaric acid	164,05	3	2	1,44	0	-5,56	-4,764
Coutaric acid	296,714	8	4	0,946	0	-6,344	-4,468
epicatechin	290,08	6	5	1,094	0	-6,728	-5,145
epicatechin_gallate	442,09	10	7	1,672	1	-7,759	-6,005
E_Viniferin	454,14	6	5	4,371	0	-8,327	-5,345
Fertaric acid	326,06	9	4	0,399	0	-6,205	-4,79
Galic_acid	170,02	5	4	0,692	0	-5,362	-4,021
Kaempferol-rutinoside	594,16	15	9	1,16	3	-7,33	-5,212
Kaempferol	286,05	6	4	1,965	0	-7,064	-5,305
Myricetin	318,04	8	6	1,115	1	-6,835	-5,424
Oleanolic acid	456,36	3	2	4,11	0	-7,877	-5,462
Polydatin	380,67	8	6	1,479	1	-7,876	-5,306
Procyanidin A2	576,13	12	9	1,48	3	-7,725	-6,129
Procyanidin B1	578,14	12	10	1,221	3	-7,882	-5,765
Procyanidin B2	578,14	12	10	1,15	3	-7,984	-6,076
protocatechuic_acid	154,03	4	3	1	0	-5,389	-3,948
Quercetin	302,04	7	5	1,448	0	-7,209	-5,261
Quercetin_3_B_D_glucoside	464,1	12	8	0,674	1	-7,696	-5,722
Resveratrol.	228,08	3	3	2,895	0	-6,802	-4,719
Rutin	610,15	16	10	0,986	3	-7,29	-5,342
Syringic acid	198,05	5	2	1,209	0	-5,373	-4,129

3.5. Effects of Rkatsiteli and Areni grape extracts on MCF-7 cell viability and growth dynamics

Treatment of MCF-7 cells with Rkatsiteli and Areni extracts produced a moderate, assay-dependent antiproliferative response (Fig. 3). In the MTT assay, Rkatsiteli modestly reduced viability at 72 h (~ 60% of cells remained viable), while Areni showed little effect (Fig. 3A). RTCA showed that both extracts reduced cell growth/index over time (Fig. 3B), and brightfield microscopy confirmed decreased cell density and confluence versus controls (Fig. 3C). The discrepancy between MTT (endpoint metabolic activity) and RTCA (continuous, label-free monitoring of adhesion, proliferation, and morphology) likely explains why RTCA detected growth inhibition for both extracts despite Rkatsiteli showing the stronger MTT effect.

Overall, the extracts appear to predominantly affect proliferation and cellular behavior rather than cause pronounced direct cytotoxicity, possibly reflecting synergistic/antagonistic interactions among the multiple phytochemicals in these crude extracts.

3.6. Effects of *Rkatsiteli* and *Areni* Grape Extracts on Oxidative Stress Markers in MCF-7 Cells

Treatment with Rkatsiteli and Areni extracts differentially affected oxidative stress markers (Fig. 4). MDA levels rose ~ 27% with Rkatsiteli ($p < 0.05$) but only slightly and non-significantly with Areni (Fig. 4A). SOD activity increased significantly in both groups (Rkatsiteli + 36.8%; Areni + 45.9%; Fig. 4B), indicating strong activation of antioxidant defenses. CAT activity fell by 23.3% with Rkatsiteli but was unaffected by Areni (Fig. 4C). Overall, both extracts predominantly modulate SOD-mediated antioxidant response, with limited/variable effects on lipid peroxidation and catalase, suggesting an adaptive response that largely preserves redox homeostasis.

3.7. Effects of *Rkatsiteli* Grape Extract on Apoptosis-Related Signaling and Cell Viability in MCF-7 Cells

ICC analysis showed that Rkatsiteli extract markedly altered apoptosis-related marker expression in MCF-7 cells (Fig. 5): BCL-2 decreased by ~ 73%, and p53 increased by ~ 39% versus DMSO control (Fig. 5A, B), indicating a shift toward pro-apoptotic signaling. As BCL-2 promotes survival by inhibiting mitochondrial apoptosis and p53 drives cell-cycle arrest/apoptosis under cellular stress, the combined BCL-2 downregulation and p53 upregulation is consistent with activation of apoptosis-associated signaling in MCF-7 cells following Rkatsiteli treatment.

4. Discussion

This integrated evaluation—combining phytochemical, biological, and computational analyses—indicates that grape stem extracts exert a moderate but biologically meaningful influence on MCF-7 cell behavior, acting predominantly through modulation of apoptotic signaling rather than acute cytotoxicity. The stronger response of Rkatsiteli relative to Areni Noir across the MTT, RTCA, and oxidative stress assays is consistent with its distinct phenolic profile—particularly its higher flavan-3-ol content—and supported its selection for downstream mechanistic (ICC) and docking analysis. The divergence between endpoint metabolic activity (MTT) and continuous real-time monitoring (RTCA) further suggests that the observed activity is predominantly cytostatic and time-dependent rather than acutely cytotoxic, a pattern frequently reported for polyphenol-rich plant extracts.

A key mechanistic finding is the coordinated modulation of apoptosis-related regulators. The shift in the balance between BCL-2 and p53 expression suggests activation of mitochondrial apoptotic signaling and cellular stress responses. Rather than inducing immediate cell death, the extract appears to sensitize cancer cells to intrinsic apoptotic stimuli by weakening anti-apoptotic defenses while enhancing tumor suppressor signaling.

The oxidative stress profile supports this interpretation. Increased superoxide dismutase activity, together with relatively stable catalase levels and only modest lipid peroxidation, indicates controlled redox perturbation rather than overt oxidative damage. This pattern is consistent with low-level ROS signaling acting as an upstream regulator of adaptive stress responses and apoptosis.

The computational analysis further supports these observations by identifying multiple phytochemicals capable of interacting with both Bcl-2 and p53. Although ε-viniferin exhibited the strongest binding affinity, its predicted toxicity limits its translational potential. In contrast, oleanolic acid and polydatin combined favorable binding with more acceptable predicted pharmacokinetic and safety profiles. At the same time, the comparison between docking and cellular findings highlights an important limitation of in silico screening, as high binding affinity does not necessarily translate into

equivalent biological activity because of factors such as membrane permeability, metabolism, compound stability, intracellular concentration, and interactions among multiple extract constituents. Given the multi-component nature of grape extracts, their biological effects are likely mediated through coordinated modulation of interconnected pathways regulating oxidative stress, mitochondrial integrity, and apoptosis rather than through single-target inhibition. This systems-level mechanism is consistent with the simultaneous alterations observed in antioxidant defenses and apoptotic markers.

In conclusion, the study highlights the biological relevance of grape-derived phytochemicals as modulators of cancer cell signaling networks rather than direct cytotoxic agents. The integration of experimental and computational approaches provides a more comprehensive understanding of their mechanism of action and underscores the importance of considering both target affinity and pharmacological feasibility in natural product research. Further fractionation and bioactivity-guided isolation will be necessary to identify the specific constituents responsible for the observed effects and clarify their synergistic interactions within the crude extract matrix.

Limitations. Several limitations should be considered when interpreting these findings. First, the biological evaluation was performed in a single cancer cell line (MCF-7); no comparison with a non-tumorigenic breast epithelial cell line was included, so the selectivity of the extracts toward cancer versus normal cells could not be established. Second, oxidative stress and apoptosis-related markers (BCL-2, p53) were assessed only for the Rkatsiteli extract, based on its stronger antiproliferative response in preliminary screening; the mechanistic basis of Areni Noir's comparatively weaker activity was therefore not directly investigated at the molecular level. Third, all bioactivity data derive from crude multi-component extracts; the individual contribution of specific constituents (e.g., oleanolic acid, polydatin, ε-viniferin) to the observed cellular effects remains to be established through bioactivity-guided fractionation or testing of isolated/purified compounds. Finally, no *in vivo* data are available, and extrapolation of these in vitro findings to physiological conditions—including compound bioavailability, metabolism, and systemic effects—requires further preclinical investigation.

5. Conclusion

This study characterized the phytochemical composition, antioxidant activity, antiproliferative effects, and molecular mechanisms of *Vitis vinifera* cv. Rkatsiteli and cv. Areni Noir stem extracts. HPLC-MS revealed a diverse polyphenolic profile in both cultivars, with Rkatsiteli enriched in flavan-3-ols and Areni Noir in gallic acid, and comparable DPPH antioxidant activity (IC_{50} 182.9 and 188.8 μg/mL, respectively). Given its stronger antiproliferative response in preliminary screening, Rkatsiteli was selected for in-depth mechanistic characterization. In MCF-7 cells, Rkatsiteli produced a moderate, time-dependent, predominantly cytostatic effect, accompanied by SOD activation, downregulation of BCL-2, and upregulation of p53, indicating engagement of pro-apoptotic signaling. Molecular docking identified ε-viniferin, oleanolic acid, and polydatin as leading BCL-2/p53-binding candidates, with oleanolic acid and polydatin showing the most favorable affinity-ADMET balance, supporting a multi-target mechanism consistent with the extracts' complex polyphenolic composition. Collectively, these winemaking by-products from Armenian grape varieties represent valuable, underexplored sources of bioactive phytochemicals with biologically relevant anticancer signaling effects, warranting bioactivity-guided fractionation and preclinical evaluation of the most promising compounds.

Abbreviations

ADMET
Absorption
Distribution
Metabolism
Excretion
and Toxicity
ANOVA
Analysis of Variance

ATCC
American Type Culture Collection
AUC
Area Under the Curve
BCL
2—B—cell Lymphoma 2
BSA
Bovine Serum Albumin
CAT
Catalase
CI
Cell Index
CO_2
Carbon Dioxide
DAPI
4'
6
Diamidino—2—Phenylindole
DMEM
Dulbecco's Modified Eagle Medium
DMSO
Dimethyl Sulfoxide
DPPH
2
2
Diphenyl—1—Picrylhydrazyl
ESI
Electrospray Ionization
GAE
Gallic Acid Equivalents
HPLC
High—Performance Liquid Chromatography
HBA
Hydrogen Bond Acceptors
HBD
Hydrogen Bond Donors
ICC
Immunocytochemistry
IC_{50}
Half Maximal Inhibitory Concentration
IgG
Immunoglobulin G
LogP
Logarithm of Partition Coefficient
MDA
Malondialdehyde
MS

Mass Spectrometry
MTT
3—(4
5
Dimethylthiazol—2—yl)—2
5
Diphenyltetrazolium Bromide
MW
Molecular Weight
OIV
International Organisation of Vine and Wine
PDB
Protein Data Bank
PDA
Photodiode Array
PFA
Paraformaldehyde
RE
Rutin Equivalents
RMSD
Root Mean Square Deviation
ROS
Reactive Oxygen Species
RTCA
Real—Time Cell Analysis
SEM
Standard Error of the Mean
SOD
Superoxide Dismutase
TFC
Total Flavonoid Content
TPC
Total Phenolic Content
UPLC
Ultra—Performance Liquid Chromatography.

Declarations

6. Data statement

The datasets used and/or analyzed during the current study are available from the corresponding author upon reasonable request.

7. Competing interests

The authors declare that they have no competing interests.

8. Funding

The research received support from the Higher Education and Science Committee of MESCS RA through research project number 24WS-1F036.

9. Ethics approval and consent to participate

Not applicable.

10. Consent for publication

All authors have read and approved the final manuscript.

11. Authors' contributions

VK conceived and designed the study, performed the HPLC–MS analysis, curated and formally analyzed the data, and drafted the manuscript. HJ performed the immunocytochemistry (ICC) experiments, contributed to data interpretation, and drafted and critically revised the manuscript. AM performed the HPLC–MS analysis, curated and formally analyzed the data, and drafted the manuscript. AsM performed the antioxidant assays and real-time cell analysis (RTCA), curated the data, and drafted the manuscript. AD performed the HPLC–MS analysis, conducted formal analysis and data interpretation, and drafted the manuscript. SH supervised the study, contributed to data interpretation, and critically revised the manuscript. NA supervised the study, performed the immunocytochemistry (ICC) analysis, contributed to data analysis and visualization, and critically revised the manuscript. All authors read and approved the final manuscript.

12. Declaration of generative AI use.

During the preparation of this work, the authors used Claude (Anthropic) in order to improve the language, readability, and clarity of the manuscript text. After using this tool, the author(s) reviewed and edited the content as needed and take full responsibility for the content of the publication.

References

1. Karastergiou A, Gancel AL, Jourdes M, Teissedre PL. Antioxidants 13, (2024).
2. *International Organisation of Vine and Wine (OIV). State of the world vine and wine sector in 2023 [Internet]. Dijon: OIV; 2024 Apr [cited 2026 Aug 19]. Available from*: https://www.oiv.int/sites/default/files/2024-04/OIV_STATE_OF_THE_WORLD_VINE_AND_WINE_SECTOR_IN_2023.*pdf*.
3. Scalbert A, Johnson IT, Saltmarsh M. *Polyphenols: Antioxidants and beyond 1–3* (2005).
4. Rockenbach II, Rodrigues E, Gonzaga LV, Caliari V, Genovese MI, Gonalves AEDSS, Fett R. Food Chem. 2011;127:174.
5. Teixeira A, Baenas N, Dominguez-Perles R, Barros A, Rosa E, Moreno DA, Garcia-Viguera C. Int J Mol Sci. 2014;15:15638.
6. Anastasiadi M, Chorianopoulos NG, Nychas GJE, Karoutounian SA. J Agric Food Chem. 2009;57:457.
7. Apostolou A, Stagos D, Galitsiou E, Spyrou A, Haroutounian S, Portesis N, Trizoglou I, Wallace Hayes A, Tsatsakis AM, Kouretas D. Food Chem Toxicol. 2013;61:60.
8. Veskoukis AS, Vassi E, Poulas K, Kokkinakis M, Asprodini E, Haroutounian S, Kouretas D. Anticancer Res. 2020;40:2025.
9. Vassi E, Veskoukis A, Tekos F, Skaperda Z, Poulas K, Haroutounian S, Kouretas D. Int J Funct Nutr 3, (2022).
10. de Araújo FF, de Paulo Farias D, Neri-Numa IA, Pastore GM. Food Chem. 338, (2021).
11. Sun S, Liu Z, Lin M, Gao N, Wang X. Front Nutr 11, (2024).
12. Schieber M, Chandel NS. Curr Biol 24, (2014).
13. Di Meo S, Reed TT, Venditti P, Victor VM. Oxid. Med. Cell. Longev. 2016, (2016).
14. Cory S, Adams JM. Nat Rev Cancer. 2002;2:647.

15. Javrushyan H, Ginovyan M, Harutyunyan T, Gevorgyan S, Karabekian Z, Maloyan A, Avtandilyan N. PLoS ONE. 2025;20:e0303736.
16. Hsu A-L, Ching T-T, Wang D-S, Song X, Rangnekar VM, Chen C-S. *The Cyclooxygenase-2 Inhibitor Celecoxib Induces Apoptosis by Blocking Akt Activation in Human Prostate Cancer Cells Independently of Bcl-2** (2000).
17. Ginovyan M, Javrushyan H, Hovhannisyan S, Nadiryan E, Sevoyan G, Harutyunyan T, Gevorgyan S, Karabekian Z, Maloyan A, Avtandilyan N. Sci Rep 14, (2024).
18. Tótha G, Barabás C, Tóth A, Kéry Á, Béni S, Boldizsár I, Varga E, Noszál B. Biomed Chromatogr. 2016;30:923.
19. Varga E, Barabás C, Tóth A, Boldizsár I, Noszál B, Tóth G. Nat Prod Res. 2019;33:1664.
20. Castejón ML, Montoya T. C. Alarcón-de-la-lastra, and M. Sánchez-hidalgo, Antioxidants 9, (2020).
21. Neelam A, Khatkar, Sharma KK. Crit Rev Food Sci Nutr. 2020;60:2655.
22. Ginovyan M, Javrushyan H, Petrosyan G, Kusznierewicz B, Koss-Mikołajczyk I, Koziara Z, Kuczyńska M, Jakubek P, Karapetyan A, Sahakyan N, Maloyan A, Bartoszek A, Avtandilyan N. Int J Biochem Cell Biology 158, (2023).
23. Kennedy JA, Waterhouse AL. *Analysis of Pigmented High-Molecular-Mass Grape Phenolics Using Ion-Pair, Normal-Phase High-Performance Liquid Chromatography* (2000).
24. Zejli H, Amrani BEL, Metouekel A, Bousseraf FZ, Fitat A, Taleb M, Abdellaoui A. Moroccan J Chem. 2024;12:361.
25. Benedec D, Hanganu D, Oniga I, Filip L, Bischin C, Silaghi-Dumitrescu R, Tiperciuc B, Vlase L. Molecules 21, (2016).
26. Ielciu I, Frédérich M, Hanganu D, Angenot L, Olah NK, Ledoux A, Crisan G, Paltinean R. Antioxidants 8, (2019).
27. Ginovyan M, Javrushyan H, Karapetyan H, Koss-Mikołajczyk I, Kusznierewicz B, Grigoryan A, Maloyan A, Bartoszek A, Avtandilyan N. Cell Biochem Funct 42, (2024).
28. Javrushyan H, Petrosyan G, Mróz M, Kusznierewicz B, Alharithi Y, Ginovyan M, Maloyan A, Avtandilyan N. FASEB J 40, (2026).
29. Ginovyan M, Gevorgyan S, Javrushyan H, Kusznierewicz B, Koss-Mikołajczyk I, Sahakyan N, Bartoszek A, Avtandilyan N. BMC Complement Med Ther (2026).

Figures

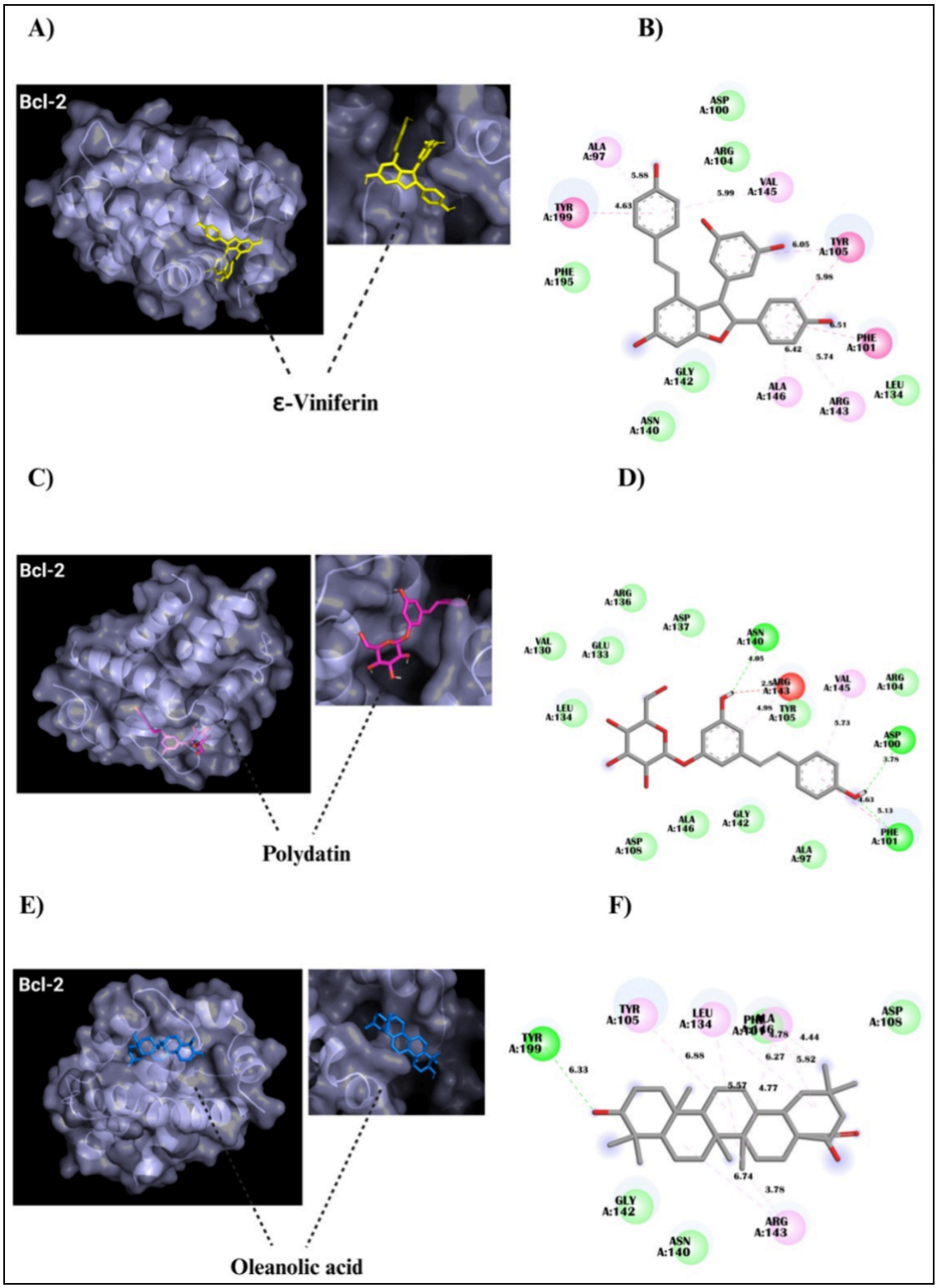


Figure 1

Molecular docking analysis of E-viniferin, polydatin, and oleanolic acid with Bcl-2. (A) Three-dimensional representation of E-viniferin bound within the Bcl-2 binding cavity. (B) Two-dimensional interaction map showing hydrophobic and aromatic contacts involved in complex stabilization. (C) Three-dimensional docking pose of polydatin within the Bcl-2 binding pocket. (D) Two-dimensional interaction diagram illustrating the amino acid residues participating in ligand binding. (E) Three-dimensional representation of oleanolic acid docked to Bcl-2. (F) Two-dimensional interaction profile

showing hydrogen bonding, hydrophobic, and π-mediated interactions contributing to stabilization of the Bcl-2–oleanolic acid complex.

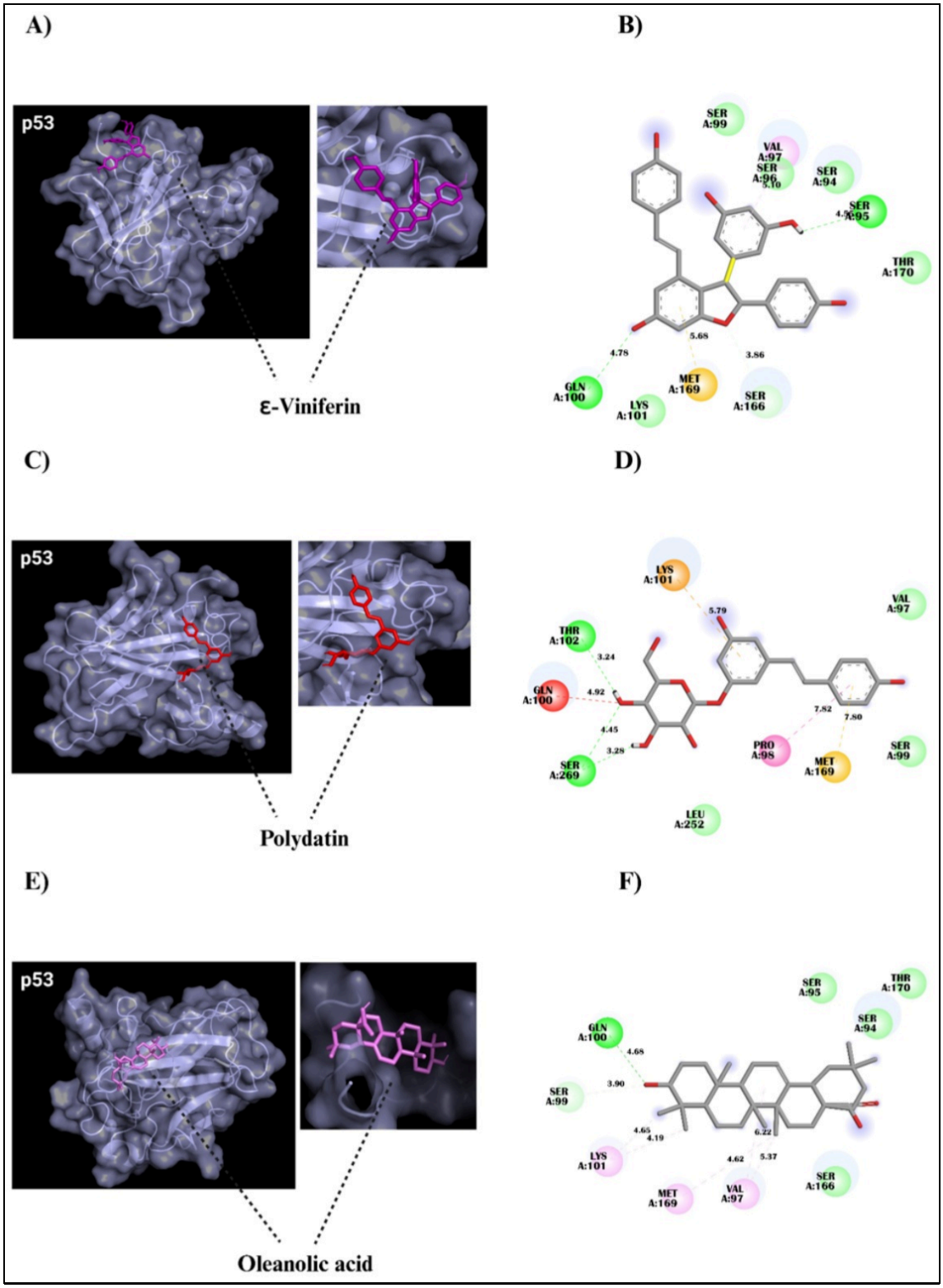


Figure 2

Molecular docking analysis of E-viniferin, polydatin, and oleanolic acid with p53.
(A) Three-dimensional representation of E-viniferin docked within the p53 binding pocket. (B) Two-dimensional interaction map showing amino acid residues involved in ligand stabilization. (C) Three-dimensional binding pose of polydatin within p53. (D) Two-dimensional interaction profile of the p53–polydatin complex, highlighting hydrogen bonds,

π–cation, π–sulfur, and hydrophobic interactions. (E) Three-dimensional docking conformation of oleanolic acid in the p53 binding site. (F) Two-dimensional interaction diagram illustrating the key contacts stabilizing the p53–oleanolic acid complex.

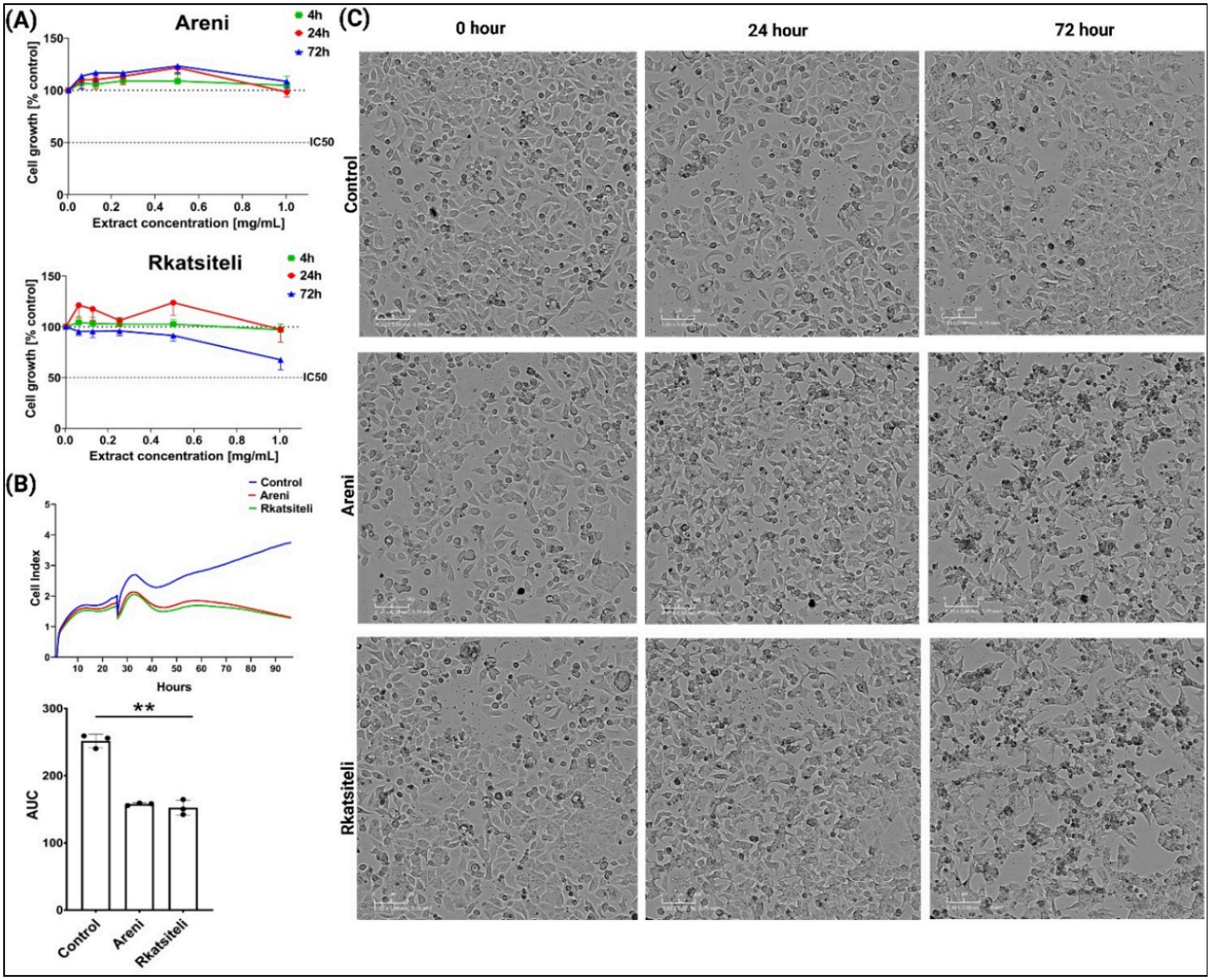


Figure 3

Cytotoxicity and real-time cell analysis of MCF-7 cells treated with Rkatsiteli and Areni noir. (A) MCF-7 cell viability was assessed by MTT assay after treatment with *Rkatsiteli and Areni* extracts at the indicated concentrations for 4, 24, and 72 h. Data are expressed as a percentage of viable cells relative to the untreated control and are presented as mean ± SEM (n = 3). (B) Real-time monitoring of MCF-7 cell index using the xCELLigence RTCA system. The top graph shows kinetic cell index (CI) curves following treatment with Rkatsiteli and Areni noir. The bottom graph presents the corresponding area under the curve (AUC) analysis, reflecting cumulative cell viability activity over the experimental period. (C) Real-time detection of cell death. Representative pictures (24 and 72 hours) are shown for untreated control cells and for cells treated with Rkatsiteli and Areni noir over the experimental period. Statistical significance was assessed using one-way ANOVA, with $p < 0.05$ considered significant. Magnification: 10×; scale bar: 100 µm.

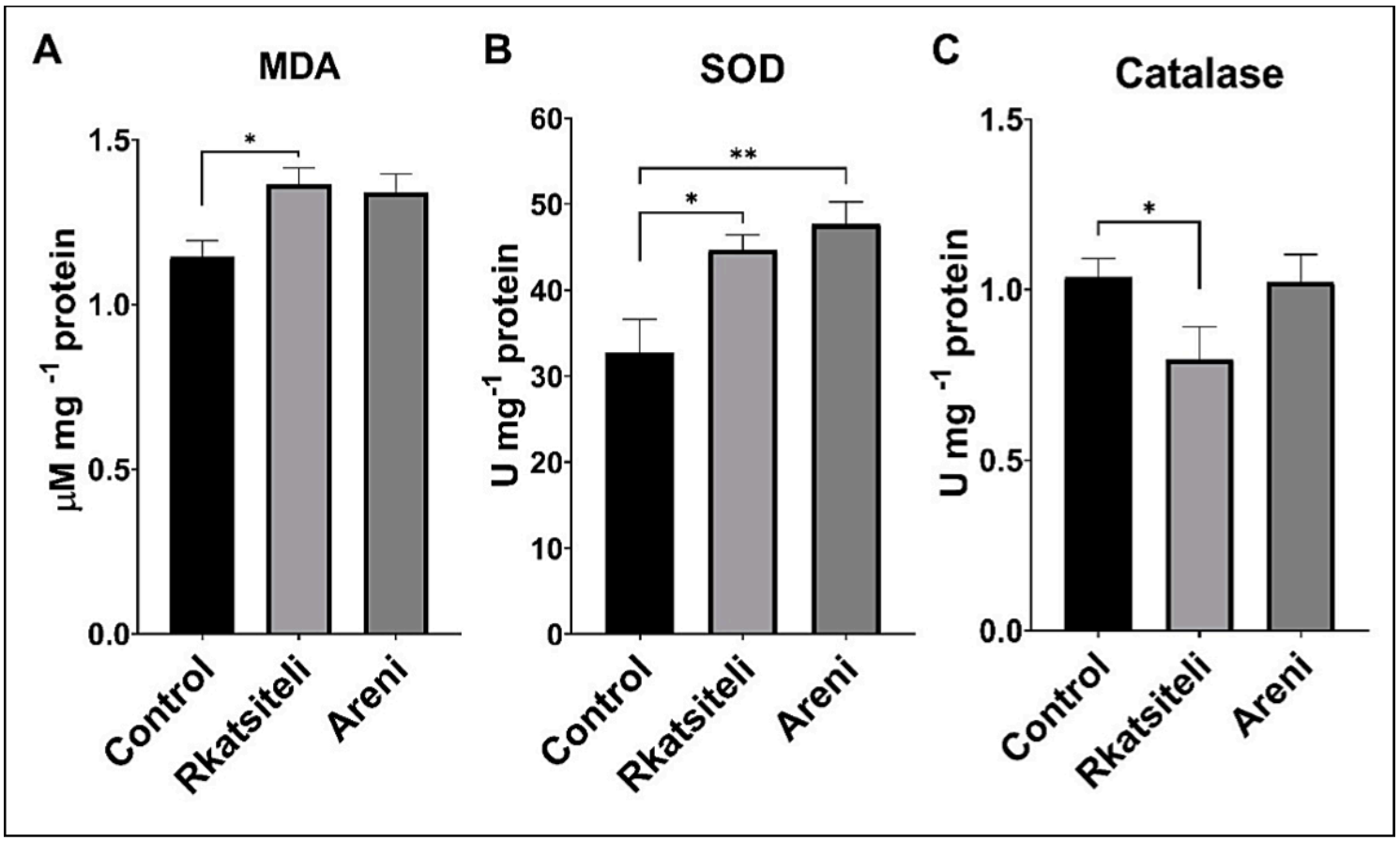


Figure 4

Changes in SOD, catalase activity, and MDA quantity in MCF-7 cells with Rkatsiteli and Areni Noir extract treatment. Results are expressed as mean ± SEM. *p < 0.05, **p < 0.01, ***p < 0.001, ****p < 0.0001.

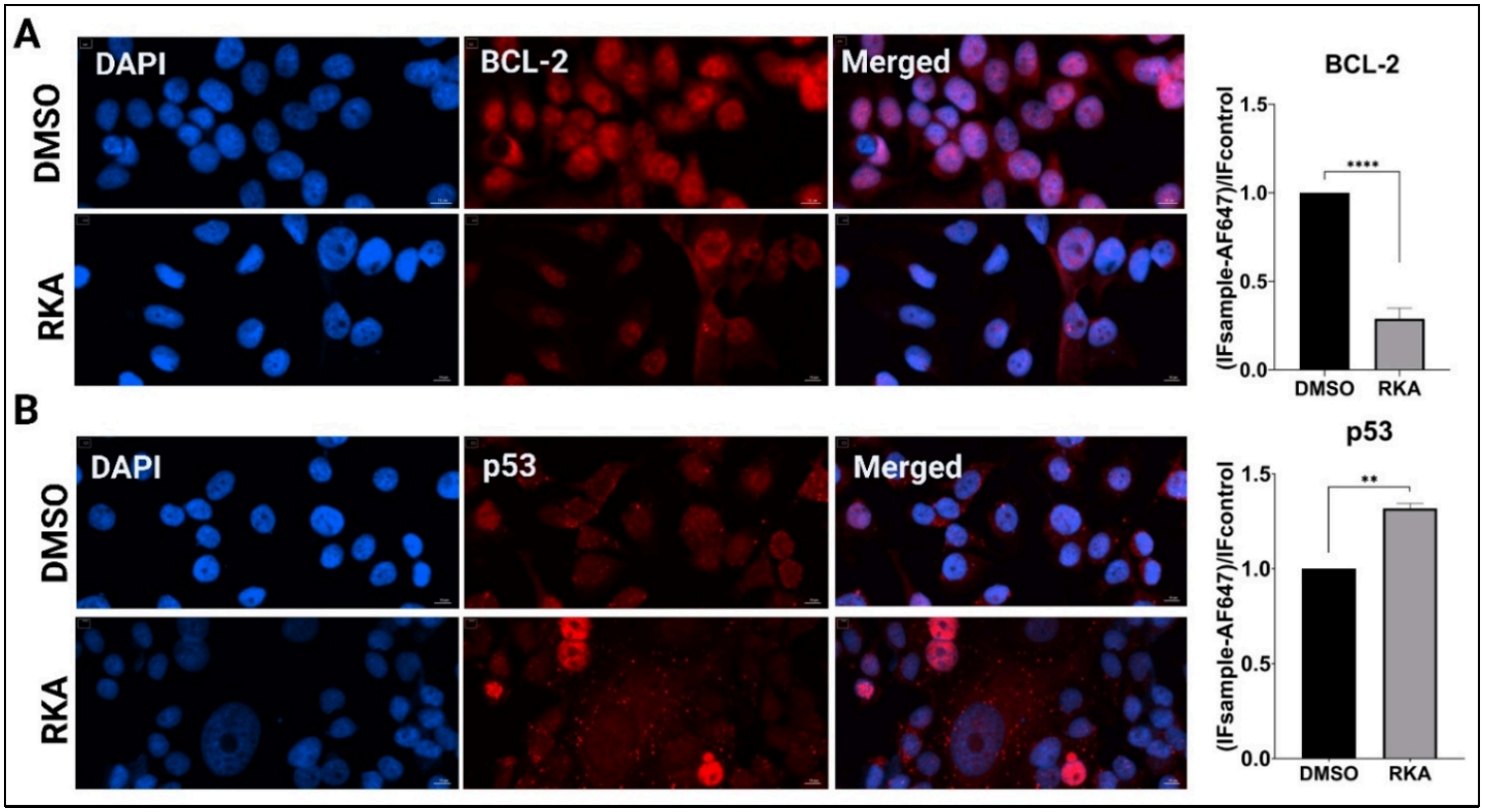


Figure 5

Comparative effects of *Rkatsiteli* grape extract (REK) on BCL-2 (A) and p53 (B) level changes in MCF-7 breast cancer cells. Representative immunofluorescence images of MCF-7 cells treated with vehicle control (DMSO) and *Rkatsiteli* grape extract. Nuclei were counterstained with DAPI (blue), whereas target proteins were detected using Alexa Fluor 647-conjugated secondary antibodies (red). Merged images are shown in the right panels. Quantification of mean fluorescence intensity normalized to vehicle-treated control cells (DMSO = 1). Data represent mean ± SEM from three independent biological experiments; in each experiment, cells were seeded in three separate wells per condition, and eight random microscopic fields were analyzed per well. The plotted values correspond to the pooled mean of all independent replicates. Statistical significance was determined by one-way ANOVA followed by multiple-comparison post hoc analysis. *p < 0.05, **p < 0.01, ****p < 0.0001; ns, not significant. Magnification: 20×; scale bar: 20 μm.